Harmonin inhibits presynaptic $Ca_v1.3$ Ca^{2+} channels in mouse inner hair cells

Frederick D. Gregory, Keith E. Bryan, Tina Pangršič, Irina E. Calin-Jageman, Tobias Moser, and Amy Lee

Supplementary Figure 1

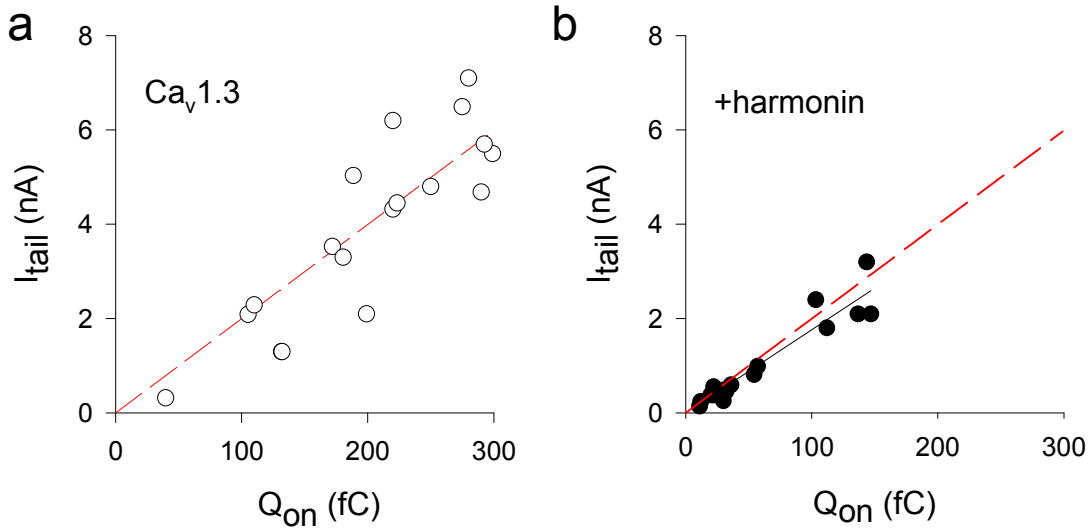

Supplementary Figure 1. Scatter plots of tail current amplitudes vs. ON gating charge in HEK293T cells transfected with $Ca_v1.3$ ($\alpha_1$1.3, β_{1b}, $\alpha_2\delta$) alone (***a***) or cotransfected with harmonin (***b***). As described for Fig.1d, the time integral of the ON gating current measured at the I_{Ba} reversal potential (+60 mV) represents the maximal gating charge (Q_{on}) and was used to reflect the number of available $Ca_v1.3$ channels. Assuming that harmonin does not affect single-channel conductance or maximum gating charge per channel, the ratio of the tail current (I_{tail}) and Q_{on} can be used to estimate the relative open probability (P_o) of the plasma membrane $Ca_v1.3$ channels. Linear regression of the I_{tail} vs. Q_{on} plots (red dashed line in ***a***, solid black line in ***b)*** revealed no significant difference (p=0.25 by ANCOVA) in slope for $Ca_v1.3$ alone (0.023±0.003) and $Ca_v1.3$+harmonin (0.018±0.001*;* regression line from ***a*** redrawn in ***b*** for comparison), which argues against an effect of harmonin on P_o.

Supplementary Figure 2

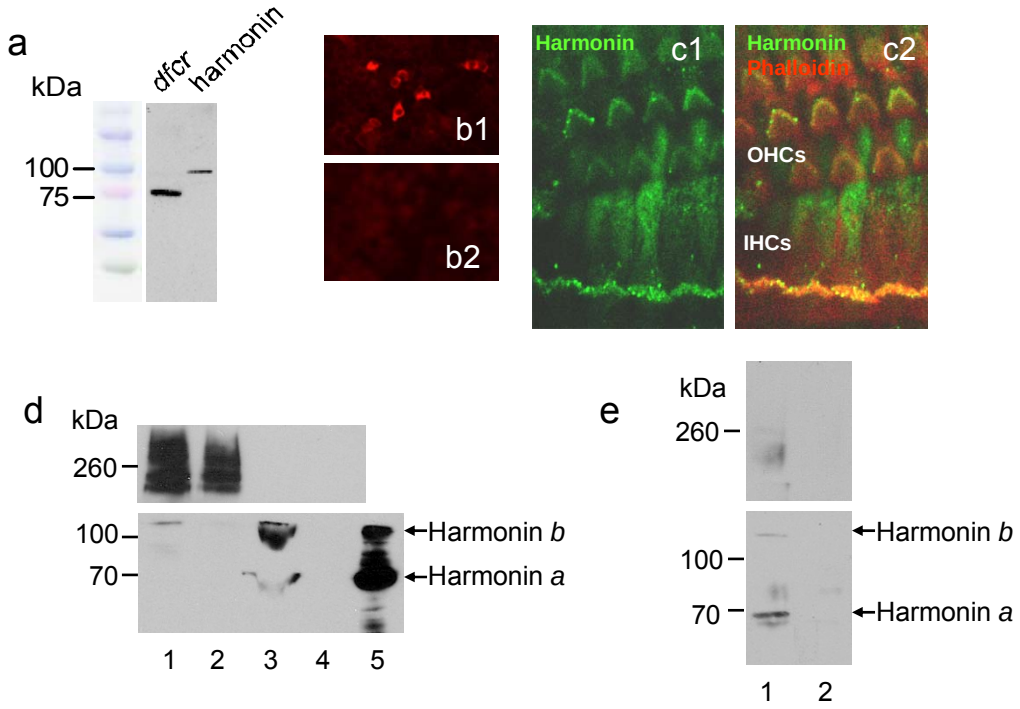

Supplementary Figure 2. Characterization of harmonin antibodies and coimmuoprecipitation of harmonin/$Ca_v1.3$ complexes. ***a-c***, Characterization of harmonin antibodies. ***a,*** Western blot of lysates from HEK293T cells transfected with GFP-tagged harmonin or *dfcr* mutant. Blot was probed with anti-harmonin and HRP-conjugated anti-rabbit antibodies. ***b***, Immunofluorescence of HEK293T cells transfected with harmonin (b1) but not in untransfected cells (b2). Cells were processed with anti-harmonin and Texas-Red conjugated secondary antibodies. ***c***, Harmonin labeling of tips of hair bundles of outer and inner hair cells (OHCs, IHCs) in whole-mount mouse Organ of Corti (c1). Tissue was double labeled with Texas-Red-phalloidin (red) and harmonin antibodies in concert with FITC-conjugated secondary antibodies (green). Regions of colocalization appear yellow in the merged image (c2).***d-e,*** Coimmunoprecipitation of $Ca_v1.3$ and harmonin from brain (**d**) and cochlea (**e**). ***d***, Goat $\alpha_1$1.3 antibodies coimmunoprecipitated harmonin *b* from WT (lane 1) but not harmonin KO mouse forebrain (lane 2). Lanes 3, 4 represent ~10% of input lysate from WT (lane 3) or harmonin KO mouse brain (lane 4). The sensitivity of $\alpha_1$1.3 antibodies was insufficient to detect $\alpha_1$1.3 in the brain lysate input. Major bands in lane 5 represent harmonin *a* and *b* variants expressed in HEK293T cells. ***e,*** $\alpha_1$1.3 antibodies (lane 1) but not control IgG (lane 2) coimmunoprecipitate primarily harmonin *a* from mouse cochlear extract. In ***d*** and ***e***, western blotting was with rabbit $\alpha_1$1.3 antibodies (top) or harmonin antibodies (bottom).

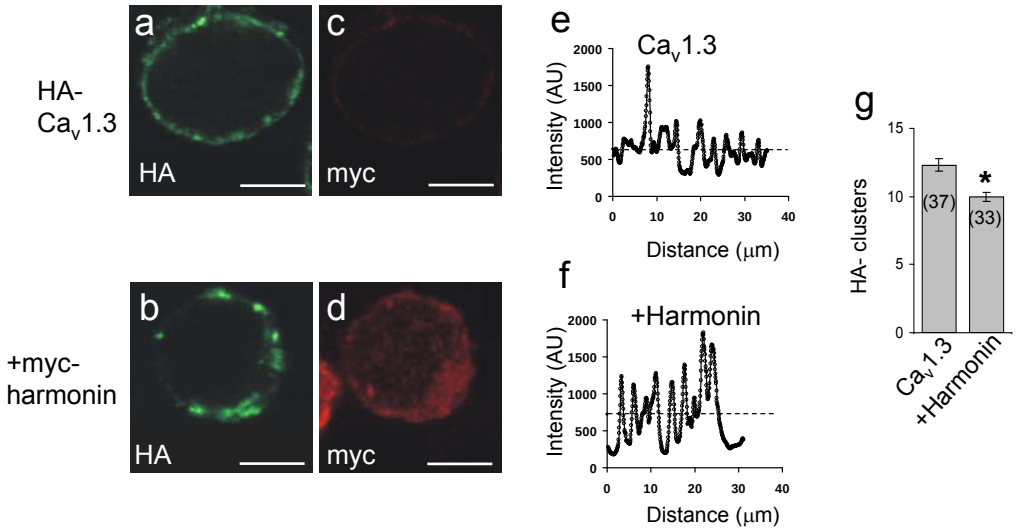

Supplementary Figure 3. Immunofluorescent measurement of surface-labeled $Ca_v1.3$ channels in transfected HEK239T cells. $Ca_v1.3$ channels with extracellular HA-epitope were transfected alone or with myc-tagged harmonin. Cells were fixed and processed first for HA labeling, followed by permeabilization and labeling with anti-myc antibodies (see supplementary methods). ***a-d,*** Confocal micrographs show continuous surface labeling in cells transfected with $Ca_v1.3$ alone (***a,c***) in contrast to cells cotransfected with harmonin (***b,d***). Scale bars, 5 μm. ***e***,***f,*** Intensity of surface HA-labeling within a cell was plotted against circumferential distance of the plasma membrane. Dashed line represents average signal intensity for the cell, above which peaks represent clusters of HA-immunofluorescence. ***g,*** From data obtained as in ***e***,***f,*** mean number of signal peaks above threshold is shown for each group. Parentheses indicate number of cells analyzed in two independent experiments. *, $p<0.05$ by t-test. Error bars represent ± S.E.M.

Supplementary Figure 4

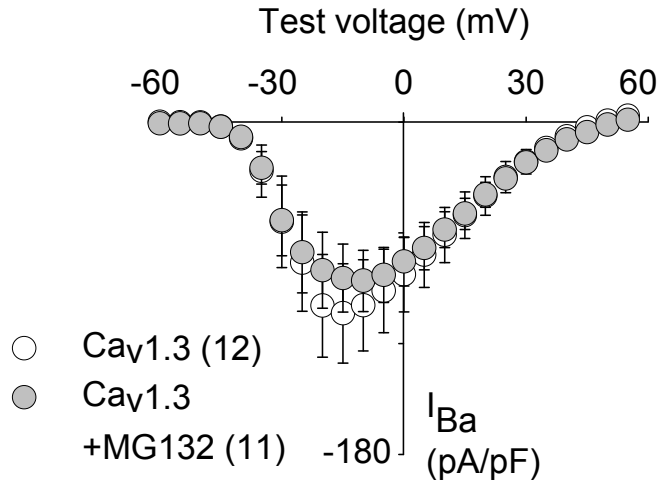

Supplementary Figure 4. MG132 does not significantly affect current density in HEK293T cells transfected with $Ca_V1.3$ alone (p=0.99 by ANOVA). Cells were transfected and treated with MG132, and current density was measured, as in Fig. 3e. Parentheses indicate numbers of cells. Errors bars represent ± S.E.M.

Supplementary Figure 5. Depiction of full length immunoblots from Western analyses. The corresponding figure panel for each immunoblot is indicated.

Supplementary Figure 5

Fig.1a

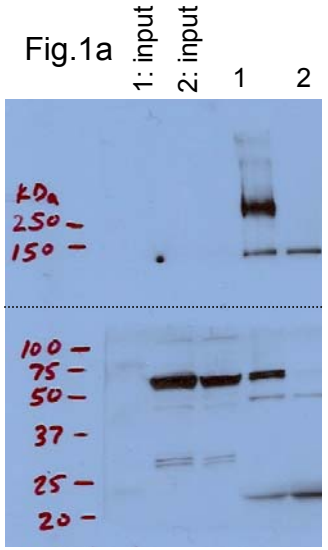

Blot

Anti-FLAG

Blot

anti-myc

1= $Ca_V1.3$+ myc-harmonin
2= myc-harmonin alone

Fig.1b

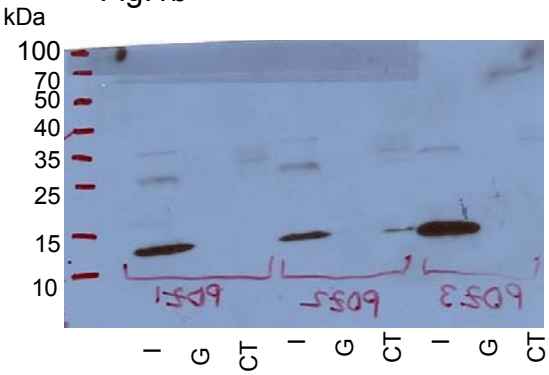

Blot

Anti-His

Fig.2a

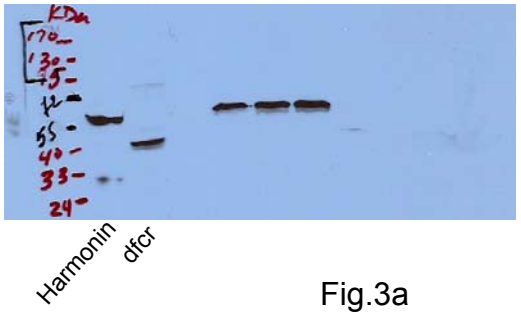

Blot

Anti-His

Fig.1e

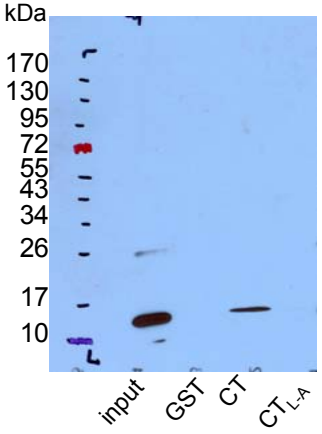

Blot

Anti-His

Fig.3a

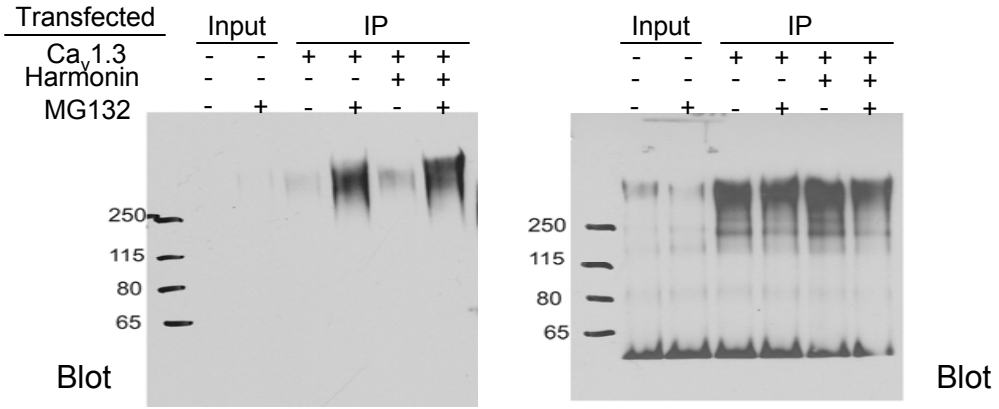

Blot

Top: anti-Ub

Blot

Bottom: anti-α1.3

Harmonin inhibits presynaptic $Ca_v1.3$ Ca^{2+} channels in mouse inner hair cells

Frederick D. Gregory, Keith E. Bryan, Tina Pangršič , Irina E. Calin-Jageman, Tobias Moser, and Amy Lee

Supplementary Table 1. Parameters for voltage-dependent activation in cells transfected with $Ca_v1.3$±harmonin.

Transfected cDNAs	$V_{1/2}$ (mV)	*k*	n
$\alpha_1 1.3/\beta_{1b}/\alpha_2\delta$	-30.3±0.76	7.6±0.26	11
$\alpha_1 1.3/\beta_{1b}/\alpha_2\delta$ +harmonin *a*	-29±0.85	7.5±0.45	11
$\alpha_1 1.3/\beta_{2a}/\alpha_2\delta$	-30.1±1.2	7.0±0.64	7
$\alpha_1 1.3/\beta_{2a}/\alpha_2\delta$ +harmonin *a*	-23±1.7*	8.3±0.4	9

Ba^{2+} currents were evoked by 20-ms pulses from -90 mV to various voltages and tail currents were measured upon repolarization to -70 mV for 2 ms. Half-maximal activation voltage ($V_{1/2}$) and slope (k) were obtained from Boltzmann fits of the normalized tail current *vs* voltage plots. *p <0.05 compared to $Ca_v1.3$ alone.

Supplementary Table 2. Parameters for voltage-dependent activation in inner hair cells from control (+/-) and *dfcr* (-/-) mice

Genotype (age)	$V_{1/2}$ (mV)	*k*	n
Control (P6-8)	-19.1±0.5	5.6±0.3	45
dfcr (P6-8)	-19.8±0.7	5.9±0.1	42
Control (P16-18)	-21.3±0.6	5.5±0.1	23
dfcr (P16-18)	-21.6±0.6	6.0±0.2	31

Ba^{2+} currents were evoked by 50-ms pulses from -75 mV to various voltages. Half maximal activation voltage ($V_{1/2}$) and slope (k) were obtained from Boltzmann fits of the current *vs* voltage plots.

Supplementary Methods

Animals

Experimental procedures using mice were approved by the Institutional Animal Care and Use Committee at Emory University, the University of Iowa, and University of Goettingen. *Dfcr* mice (Jackson Laboratories, Bar Harbor, ME) were characterized previously [1] and bred on a Balb/C background. Experiments involving *dfcr* mice were performed blind to genotype.

Antibodies

Goat and rabbit $\alpha_1$1.3 antibodies were described previously [2]. Rabbit $\alpha_1$1.3 (1-22) antibodies were generated by a commercial source against a peptide containing amino acids 1-22 (MQHQRQQQEDHANEANYARGTR) of rat $\alpha_1$1.3. Rabbit harmonin antibodies were targeted to a GST-fusion protein containing amino acids 1-89 of rat harmonin. The antisera were generated by a commercial source (Covance, Princeton, NJ) and affinity purified before use.

Binding assays

Pull-down and coimmunoprecipitation experiments were performed as described previously [2]. GST-$\alpha_1$1.3 CT proteins were immobilized on glutathione beads and incubated with purified his-tagged harmonin or harmonin-transfected HEK293T cell lysates at 4 °C for 1-2 h. Beads were washed three times with ice-cold binding buffer (1 ml) and bound proteins were detected by Western blotting with anti-his (1:1000 dilution, Santa Cruz Biotechnology, Santa Cruz, CA) or anti-myc (1:1000 dilution, Sigma-Aldrich, St. Louis, MO).

For coimmunoprecipitation from transfected HEK293T cells in Fig.1a, lysates were incubated with anti-FLAG-sepharose beads (M2-sepharose, Sigma-Aldrich, St. Louis, MO, 50%

slurry) for 4 h, rotating at 4 °C. After three washes with lysis buffer, proteins were eluted with SDS-containing sample buffer and subjected to SDS-PAGE. Coimmunoprecipitated proteins were detected by Western blotting with antibodies against FLAG or myc epitopes (Sigma-Aldrich, St. Louis, MO). For coimmunoprecipitation from mouse brain (Supp.Fig.2d), the forebrains of control and harmonin KO mice (P21 Ush1c+/- or Ush1c-/- mice, respectively [3]) were homogenized in RIPA buffer and subject to centrifugation at 19,745 x *g* in a microcentrifuge for 20 min at 4 °C. For coimmunoprecipitation from cochlear tissue (Supp.Fig.2e), 16 cochleas from P24 mice were dissected and homogenized in RIPA buffer. Lysates (~3-4 mg protein for forebrain, ~0.5-1 mg for cochlea) were incubated with goat $\alpha_1$1.3 antibodies and protein G-sepharose overnight, rotating at 4 °C. After three washes with RIPA buffer, proteins were eluted with SDS-containing sample buffer and subjected to SDS-PAGE. Coimmunoprecipitated proteins were detected by Western blotting with rabbit $\alpha_1$1.3 (1-22) or harmonin antibodies.

Ubiquitination assay

HEK293T cells transfected with (1) Ca_v1.3+EGFPN1 or (2) Ca_v1.3+EGFP-harmonin were incubated for 18-24 h with MG132 (5 μM, Calbiochem) or DMSO control and prepared for immunoprecipitation with $\alpha_1$1.3 antibodies as described above. Approximately 300 μg of cellular protein obtained from each lysate was incubated with 3 μg of $\alpha_1$1.3 antibodies in the presence of protein A sepharose beads. Binding reactions were incubated overnight with continuous mixing at 4°C. The beads were washed four times with 1 ml of ice-cold lysis buffer (TBS, pH 8.0, 1% TX100, Roche complete protease inhibitors) and bound proteins were eluted, resolved by SDS-PAGE (4-12% Tris-Bis gradient gel, Invitrogen, Gaithersburg, MD), and transferred to nitrocellulose. Western blot analysis was with mouse monoclonal anti-Ub (BD

Pharmigin, San Diego, CA; 1:2000) or rabbit $\alpha_1$1.3 antibodies (1:4000). Blots were processed with HRP-conjugated anti-mouse or rabbit IgG secondary antibodies, respectively, (GE Healthcare, Piscatway, NJ; 1:4000) and ECL reagent (Thermo Scientific, Waltham, MA). Western blotting with mouse monoclonal β-actin antibodies (Sigma) was to confirm relatively equal levels of protein input between groups. Differences in signal intensity were determined by densitometric analysis using a Canon LIDE 200 scanner and ImageJ (NIH) software. For each experiment, the signals due to anti-ubiquitin antibodies (ubiquitinated channel) or anti-$\alpha_1$1.3 antibodies (total channel) were first normalized to the most intense signal on the blot, which compensated for differences in film exposure between experiments. A ratio between the normalized ubiquitin and $\alpha_1$1.3 signals was then interpreted as the ubiquitinated fraction of total channels per group. These values are reported as relative intensity in Fig.4b. Quantification and statistics (one-way ANOVA) is based on results from four independent transfections and sample preparations.

Immunofluorescent detection of cell surface Ca_v1.3 channels

HEK293T cells transfected with Ca_v1.3 channels with extracellular HA epitope [4] alone or cotransfected with myc-harmonin were plated on poly-D-lysine (50 μg/ml, Sigma)-treated glass coverslips, fixed with 4% paraformaldehyde/PBS for 15 min at room temperature, blocked for 30 min in blocking buffer (BB: 5% normal goat serum, 0.5% BSA, PBS), and incubated with rat HA antibodies (1:1000 in BB, Roche). Secondary detection was with Alexa 488-tagged anti-rat antibodies (1:1000 in BB, Invitrogen). The cells were then permeabilized with 0.1% triton X-100 in BB and processed for anti-myc fluorescence with mouse anti-myc antibodies (1:4000, Sigma) and Alexa 568-tagged anti-mouse secondary antibodies (1:1000 in BB, Invitrogen). Double-

labeling with myc antibodies permitted detection of cells expressing both $Ca_v1.3$ and harmonin. Coverslips were mounted to glass slides using Dako medium (Dako, Carpinteria, CA, USA) and sealed with finger nail polish. Single-plan confocal images were acquired using a Fluoview FV1000 confocal scanner mounted on an upright microscope (BX61WI) equipped with an UPlanFL 1.3 NA, 100x oil-immersion objective and the following laser sources: 30 mW Multi-Ar, 1 mW HeNe, and 20 mW 635 nm diode (all Olympus). Image analysis was performed using ImageJ (NIH) software. The fluorescence intensity corresponding to the surface labeled HA-$Ca_v1.3$ was selected as the region of interest using the ROI freehand tool and the width of line was adjusted to 18. Fluorescence intensities were plotted against distance and a threshold was set as the average fluorescence intensity for that particular cell. A mathematical filter (running average of five signal intensities preceding and following a given point) was applied to the data to suppress noise and identify peaks representing surface $Ca_v1.3$ channels (Supp. Fig.3e,f). The number of peaks greater than or equal to the threshold were counted, averaged, and compared between groups (Supp.Fig.3g). Quantification and statistical analysis were based on results from two separate transfections and at least four independent sample preparations.

Immunofluorescence of mouse Organ of Corti

Freshly dissected apical cochlear turns of P8-P9 mice were fixed with 99.8% methanol (Sigma Aldrich) for 20 min at -20°C for synaptic labeling or 4% paraformaldehyde for 20 min at room temperature for hair bundle labeling. The tissue was washed three times for 10 min in tris-buffered saline (TBS) and non-specific sites were blocked by incubating in blocking buffer (30% normal donkey serum in TBS) for 2 h at room temperature. For the synaptic double-labeling experiments, the stringent blocking conditions were necessary to reduce non-specific antibody

binding, but also may have reduced the extent of specific labeling. For this reason, quantitative analyses may have underestimated the extent of synaptic harmonin labeling, but since the same procedure was used for P6-8 and P16-18 tissue, the relative difference between the age groups should not have been affected. Primary antibodies (rabbit anti-harmonin, 1:50, or rabbit anti-$\alpha_1$1.3, 1:100; and mouse anti- CtBP2, 1:100, BD Biosciences, San Jose, CA, USA) were applied overnight at 4 °C. Secondary antibodies (rhodamine-coupled donkey anti-mouse, 1:200, and biotin-conjugated donkey anti-rabbit antibody, 1:1,000; Jackson ImmunoResearch, West Grove, PA) and FITC-coupled streptavidin (1:1,000; Sigma Aldrich) were applied sequentially each for 1.5 h at room temperature. All antibodies were diluted in blocking buffer and incubations took place in a humidified chamber. Between incubations, tissue was washed 6 times for 5 min each in TBS. The tissue was coverslipped on glass slides in mounting medium (Dako, Carpinteria, CA, USA) and analyzed with a LSM 510 (Zeiss, Oberkochen, Germany) or Fluoview 1000 confocal microscope (Olympus, Center Valley, PA) with a 63x oil immersion objective. Fluorescence was monitored with 488 nm (argon) and 543 nm (helium–neon) laser excitation and 500–550 and 565–615 nm bandpass filters. Optical sections (0.5 μm) were taken from the apical to basal surface of IHCs and projected along the z-axis using Zeiss LSM Image Browser or Olympus Fluoview software. Processed images were edited for display with Adobe Photoshop and Macromedia Freehand software.

Electrophysiological recordings

For transfected cells, whole-cell patch-clamp recordings were acquired 24-36 h post-transfection with a HEKA Elektronik (Lambrecht/Pfalz, Germany) EPC-8 or EPC-9 patch-clamp amplifier. Data acquisition and leak subtraction using a P/-4 protocol were done with Pulse software (HEKA Electronik). External recording solution contained (in mM): 150 Tris, 1 $MgCl_2$, and 10

$BaCl_2$. Internal solution contained (in mM): 140 *N*-methyl-D-glucamine, 10 HEPES, 2 $MgCl_2$, 2 Mg-ATP, and 5 EGTA. The pH of both solutions was adjusted to 7.3 with methanesulfonic acid. Electrode resistances were 1-2 MΩ in the bath solution, and series resistance was~2-4 MΩ, compensated 60- 80%.

For whole-cell patch-clamp recordings of IHCs, cochlear tissue was dissected from mice (P6-18) in MEM/Glutamax-1 (Invitrogen, Gaithersburg, MD)) supplemented with 10 mM HEPES at room temperature and were kept up to 18 hours at 37°C prior to recording. IHCs in the apical cochlear turn were visualized on an upright microscope (BX51WI, Olympus) with a 40X water-immersion objective with DIC optics. The basolateral membrane of IHCs was patch-clamped with electrodes pulled from thick-walled borosilicate glass capillaries (1B150F, Warner Instruments, Camden, CT). The internal solution contained (in mM): 120 Cs-gluconate, 80 CsCl, 0.1 $CaCl_2$, 4 MgATP, 5 HEPES and 5 EGTA; pH was adjusted to 7.35 with CsOH; osmolarity~ 305 mOsm. External solution contained (in mM): 105 NaCl, 5.8 KCl, 10 CsCl, 55 TEA-Cl, 10 $BaCl_2$), 1 MgCl, 10 glucose and 10 HEPES supplemented with MEM Vitamins and Amino Acids at 1X; pH was adjusted to 7.4 with TEA-OH; osmolarity~ 320 mOsm. On the day of recording, 4-aminopyridine (4 mM), apamin (0.3 mM) and TTX (0.5 mM, for P6-8 IHCs) were added to the external solution. Electrode resistances were 2.5-5.5 MΩ in the external solution. Data were acquired with HEKA EPC-9 or EPC-10 amplifiers controlled by Patchmaster software (HEKA Elektronik, Lambrecht, Germany). Leak subtraction was done online with a P/6 protocol. Series resistance was compensated with the patch clamp circuitry (50-70%); average uncompensated series resistance was 12.9 ±0.6 (n = 89). Currents were low-pass filtered at 5 kHz and sampled at 20 kHz except for VDF measurements, where currents were filtered at

2.9 kHz and sampled at 10 kHz. Voltages were not corrected for the liquid junction potential of -7 mV in the external recording solution.

Confocal Ca^{2+} imaging was performed with a Fluoview 300 confocal scanner mounted on an upright microscope (BX50WI) equipped with a 0.9 NA, 60x water-immersion objective (all Olympus). A 50 mW, 488 nm solid state laser (Cyan, Newport-Spectraphysics) was used for excitation of Fluo-5N (emission filter 510 long-pass (LP)) and a photomultiplier tube (R3896 PMT, Hamamatsu) was used for fluorescence detection. Ca^{2+} microdomains were identified in xy-scans during 200 ms long depolarizations (0.5% of maximum laser intensity) and further characterized using spot detection ("point scan" mode of the confocal scanner). Spot detection measurements (0.05% of maximum laser intensity, effective sampling rate of 1.85 kHz) were made at the center of a Ca^{2+} microdomain as well as at the 4 directly neighbouring pixels on each side of the center along each direction of the X- and Y-axis (130 nm spacing between the neighbouring recording locations and the center) and repeated 5 times for each pixel. Only the maximum amplitude response was further analyzed. PMT dark current was subtracted for all measurements. Data are presented as mean and standard deviation. The internal solution contained (in mM): 115 Cs-glutamate, 13 TEA-Cl, 1 $MgCl_2$, 1 $CaCl_2$, 10 EGTA, 2 ATP-Mg, 0.3 GTP-Na, 20 HEPES (pH adjusted with CsOH to 7.2, osmolarity ~ 295 mOsm) and 0.4 Fluo-5N (penta-K^+salt; Invitrogen). The external solution contained (in mM): 102 NaCl, 35 TEA-Cl, 2.8 KCl, 5 $CaCl_2$, 1 $MgCl_2$, 10 HEPES, 1 CsCl, 11.1 D-glucose (pH adjusted with NaOH to 7.2, osmolarity ~ 300 mOsm). An EPC-9 amplifier controlled by "Patchmaster" software (HEKA Elektronik, Lambrecht, Germany) was used for measurements.

Data Analysis

Electrophysiological data were analyzed with Igor (Wavemetrics, Portland, OR), Microsoft Excel, or Origin (Microcal, Northampton, MA). Average data are expressed as mean ± SEM unless indicated. I-V relationships were fit with the following equation: $I = G(V - E)/\{1 + \exp[(V - V_{1/2})/k]\}$ where G is conductance, V is test potential, E is apparent reversal potential, $V_{1/2}$ is potential of half activation, k is the slope factor. For current density plots, peak current amplitudes were normalized to whole-cell capacitance. *On* gating charge was measured by integrating the gating charge movement for the first 1.5 ms after a pulse from -90 mV to the reversal potential for the ionic current. Tail current amplitudes were recorded after repolarization to -70 mV after each test pulse. Statistical analyses were as indicated.

1. Johnson, K.R., *et al. Hum Mol Genet* **12**, 3075-3086 (2003).
2. Calin-Jageman, I., Yu, K., Hall, R.A., Mei, L. & Lee, A. *J Neurosci* **27**, 1374-1385 (2007).
3. Tian, C., *et al. Brain Res* **1328**, 57-70.
4. Jenkins, M.A., *et al. J Neurosci* **30**, 5125-5135 (2010).